



# Kinetics of reactive wetting of graphite by liquid Al and Cu–Si alloys

Di ZHANG<sup>1</sup>, Ding-yi ZHU<sup>1</sup>, Teng ZHANG<sup>1</sup>, Qin-feng WANG<sup>1,2</sup>

1. College of Materials Science and Engineering, Fuzhou University, Fuzhou 350108, China;

2. College of Mechanical and Energy Engineering, Jimei University, Xiamen 361000, China

Received 4 September 2014; accepted 22 January 2015

**Abstract:** In order to reveal the physical essence of the spreading process of reactive wetting, a sort of model of energy to explain the driving force and wetting mechanism was presented. The reactive wetting of molten Al and Cu–Si on graphite was studied by a modified sessile drop method under a vacuum, in which the contact angles were measured by ADSA software. The thermodynamic and kinetic processes of the typical reactive wetting were focused on, the thermodynamic equations of energy relations were derived, the interfacial energy of graphite and solid–liquid interfacial energy versus time at the triple line were calculated, and the dynamics model of interface energy is established. The presented dynamics model is verified by means of experimental results, and it is shown that solid–liquid interfacial energy decreases with time in exponential relationship. It provides a new method for reference to explain the process from the angle of energy.

**Key words:** reactive wetting; solid–liquid interfacial energy; contact angle; graphite; interface reaction

## 1 Introduction

A great interest has been triggered that the wetting of liquid metal on metallic or ceramic substrate is accompanied by reactions between the liquid and solid phases, and how to explain its wetting phenomenon of liquid metal on the substrate is a puzzle in material science and physical science. There are numerous researchers who studied reactive wetting dynamics, and some spreading kinetic models are obtained to describe process of reactive wetting system, for instance, the semi-empirical formula by GENNES [1], the fluid dynamics model by STAROV et al [2], the molecular dynamics model by BLAKE and HAYES [3], the characteristic equation of the reaction-limited spreading model by DEZULLUS et al [4], and the diffusion-limited model by MORTENSEN et al [5]. Coincidentally, most dynamics models of them show only relationship between contact angle ( $\theta$ ) or spread radius ( $R$ ) and time from the macro point of view, and are lack of clear description of their energy changing or wetting mechanism is rarely given essentially.

The physical interpretation of metal/graphite system case is very important in several domains of material

science, for instance in brazing of graphitic materials or in processing of graphite–metal compacts. Despite the large number of studies on the interfacial properties of the metals/graphite couples [6,7], there is still lack of clear description of their wetting kinetics at the present time. In this work, typical reaction-limited spreading is selected and the relationship between the natural logarithm of driving force (which is expressed by the difference between instantaneous interfacial energy and the equilibrium interfacial energy) and time is found to be linear, and the kinetic model built in this work is presented for the first time to describe solid–liquid interfacial energy with time in reaction-limited wetting. The experimental results conform to the dynamic expression.

## 2 Experimental

High purity (99.99%) graphite plate with an ash content less than  $100 \times 10^{-6}$  and dimensions of 20 mm  $\times$  20 mm  $\times$  4 mm was used as substrates, and it was mechanically polished by diamond pastes to a mirror finish. The purities of Al, Si and Cu employed were 99.999%. The Cu–Si alloys with Si contents of 30%, 40% and 50% (mole fraction) in nominal compositions

were prepared by arc-melting in argon (99.999% purity) atmosphere. The alloys were melted and turned in a water-cooled copper crucible for more than four times to ensure compositional homogeneity, and then they were cut into small cubic pieces for the wetting experiment. After that, all cubic pieces were polished into  $3\text{ mm} \times 3\text{ mm} \times 3\text{ mm}$  cubes.

The wetting experiments were studied by a modified sessile drop method, as detailed in Ref. [8]. Subsequent wetting was performed at a constant temperature in the vacuum environment ( $10^{-4}\text{ Pa}$ ) [9]. The characteristic of the modified sessile drop method is that the cubic alloy and the substrate were separated before testing. The graphite was placed horizontally in a vacuum chamber, and the small cube was stored in a stainless-steel tube outside the chamber, which connected an alumina dropping tube with a flexible connector. Once the desired testing temperature of the chamber is reached, the cubic can be delivered to the graphite surface through the stainless-steel. For instance, Fig. 1 shows that the Cu–30%Si (mole fraction) alloy piece was placed over the graphite at 1423 K.

Then the drop profiles were filmed by a high resolution ( $1504 \times 1000$  pixel) charge-coupled device camera. The contact angles were measured from the drop profiles by a high resolution charge-coupled device camera.

### 3 Result

The spreading kinetics of Al and Cu–Si alloys on vitreous carbon using the dispensed drop technique was studied by EUSTATHOPOULOS et al [10, 11], and both of them are typical reaction wetting system. In order to avoid perturbation on the  $\theta(t)$  curve, an improved sessile drop method was used in Ref. [8].

A plot of the variation of contact angle versus time for an experiment conducted at 1273 K for pure Al on graphite is given in Fig. 2. According to the figure, the wetting curve can be described as three stages: spontaneous spreading stage, reaction-limited spreading stage, diffusion-limited spreading stage. The second and third stages were presented in Ref. [12].

The first stage corresponds to spontaneous spreading of non-reactive wetting during which the contact angle decreases from  $180^\circ$  to  $150.76^\circ$  ( $\theta_0$ ) with a time very close to zero where the initial angle is  $150.76^\circ$ . The second stage ( $t_0 < t < t_N$ ) spreading occurs rapidly with time. In this stage, the contact angle decreases from  $150.76^\circ$  to  $64.04^\circ$  ( $\theta_F$ ) with a spreading rate which decreases continuously. The third stage ( $t_N < t < t_F$ ) is strictly linear, during which the contact angle decreases slightly (about  $3^\circ$ ). Similar spreading curves were obtained for Cu–Si alloys (Fig. 3) on graphite.

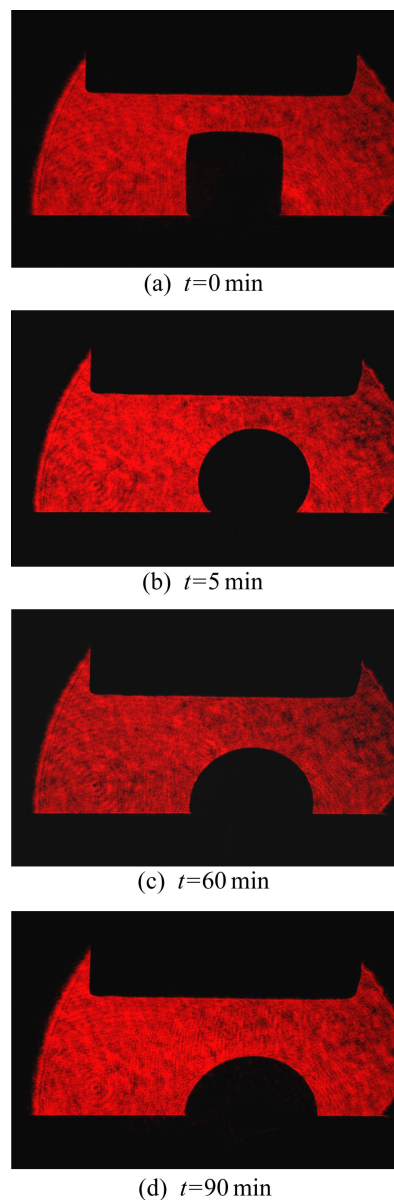


**Fig. 1** Different stages of Cu–30%Si alloy on graphite at 1423 K: (a) Initial configuration; (b) Drop formation; (c), (d) Wetting

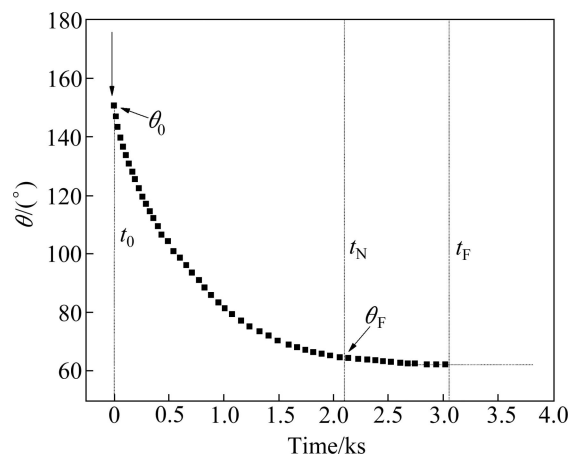


**Fig. 2** Contact angle versus time for pure Al on graphite by modified sessile drop method under vacuum at 1273 K

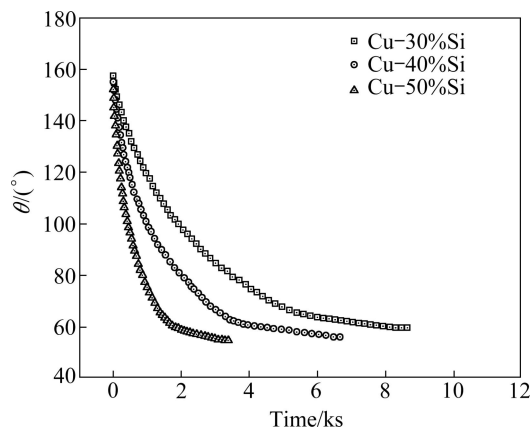


**Fig. 3** Contact angle versus time for Cu–Si alloys on graphite by modified sessile drop method under vacuum at 1423 K

Figure 3 shows that an increase in Si content produces a strong acceleration of Cu–Si alloy droplets on graphite at the same temperature and the decrease in spreading time  $t_F$  which is the time needed to reach the wetting equilibrium from more than 8000 s for Cu–30%Si to 3500 s for Cu–50%Si.

## 4 Discussion

### 4.1 Modeling for thermodynamics

#### 4.1.1 Infinite and finite solid–liquid interface of non-reactive systems

In general, two types of dynamic wetting can be distinguished, such as spontaneous wetting and forced wetting [13], and the spontaneous wetting is studied in this work. Infinite ideal solid interface is shown in Fig. 4(a), and the equilibrium contact angle of liquid on solid is  $\theta_1$ , which is used to define the wetting behavior of the liquid by many researchers. It obeys the classical elastic equation:

$$\sigma_{SV} = \sigma_{SL} + \sigma_{LV} \cos \theta_1 \quad (1)$$

where  $\sigma_{SV}$  is the solid–vapour surface energy,  $\sigma_{SL}$  is the solid–liquid interfacial energy, and  $\sigma_{LV}$  is the liquid–vapour interfacial energy.

It is commonly acknowledged that Eq. (1) cannot be solved, because only  $\sigma_{LV}$  and  $\theta_1$  can be measured by some experiments, of which commonly used methods are sessile drop method, levitating drop method and maximum bubble pressure method. In order to solve this problem, ZHU et al [13,14] introduced an ideal solid surface model for non-reactive system on the basis of the slender pillars on lotus leaf [15], as shown in Fig. 4(b). From Fig. 4(b), we can transform infinite solid interface to finite solid interface. The angle between the L–V interface and S–L interface is  $\theta_2$ , the numerical range of the contact angle of any liquid phase on the limited solid phase surface follows the inequality  $90^\circ \leq \theta_2 \leq 180^\circ$ .

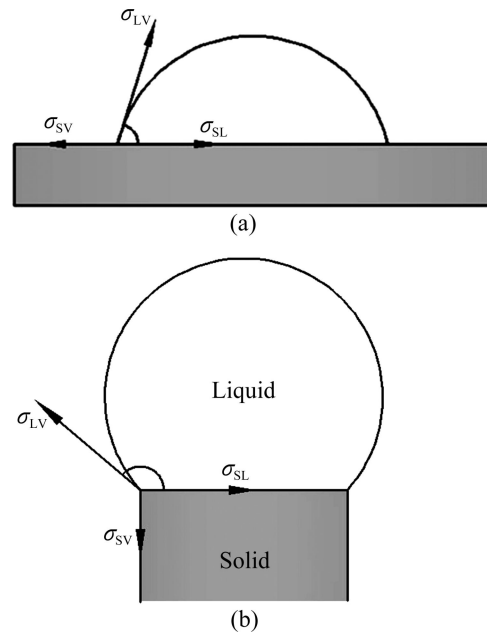


**Fig. 4** Distribution of interfacial energies at ideal infinite solid interface (a) and at ideal finite solid interface transformed from former (b)

In the horizontal and vertical direction of the finite system (Fig. 4(b)), the relation of interfacial energies is

$$\sigma_{SL} = -\sigma_{LV} \cos \theta_2 \quad (2)$$

$$\sigma_{SV} = \sigma_{LV} \sin \theta_2 \quad (3)$$

By combining Eq. (1) and Eq. (3), the following expression of the two angles is derived in Ref. [15]:

$$\cos \theta_1 = \sin \theta_2 + \cos \theta_2 \quad (4)$$

It can be simplified as

$$\sin 2\theta_2 = -\sin^2 \theta_1 \quad (5)$$

#### 4.1.2 Solid–liquid interfacial energy versus time of reactive systems

Reactive wetting at high temperature is a relatively complicated physical and chemical phenomenon. Strictly speaking, there are three types of wetting mechanism according to the essence of the driving wetting, such as dissolutive wetting [16, 17], adsorption wetting [18] and reaction wetting [4, 19]. Dissolutive wetting was studied and modeled by WARREN et al for a liquid metal B on solid metal A system at room temperature. According to the thought of these authors, the approach to equilibrium occurs in three stages when a droplet of molten B is placed on pure solid A, as shown in Figs. 5(a)–(d).

In the first stage (Figs. 5(a) and (b)), non-reactive spreading takes place in a short time  $t_0$  ( $t_0 \approx 10^{-2}$  s), the effect of dissolution on the macroscopic morphology is negligible in this stage. The contact angle  $\theta_0$  at  $t = t_0$  is nearly equal to the angle of elastic equation. According to the model, we can transform infinite system (Fig. 5(b)) to

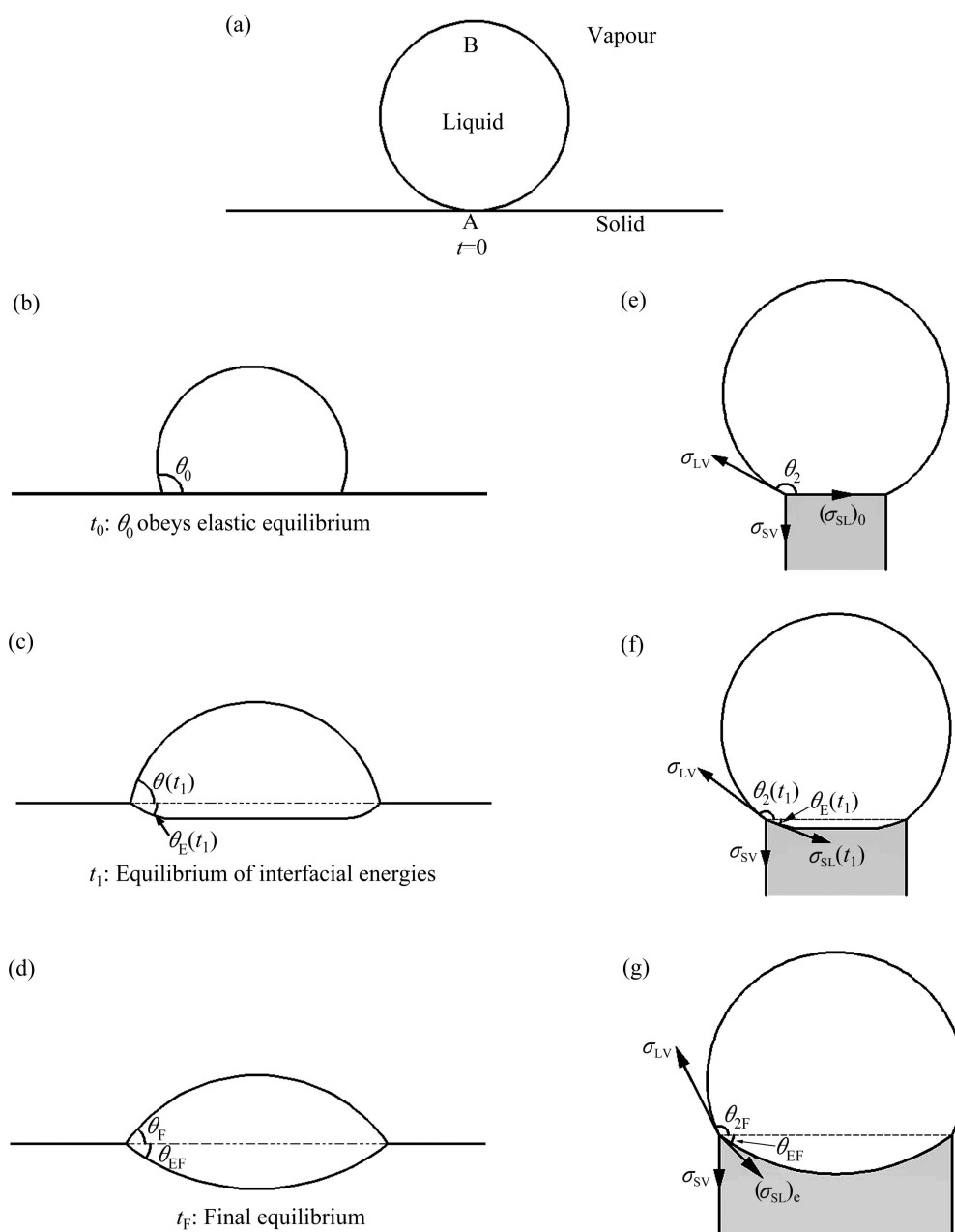


**Fig. 5** Wetting progress: (a) Initial stage; (b, c, d) Approach of elastic, instantaneous and final equilibrium in sessile drop configuration, according to Ref. [21], respectively; (e, f, g) Finite systems transformed from (b), (c) and (d), respectively

finite system (Fig. 5(e)). By combining Eqs. (2)–(4), the following expression Eq. (6) of two interfacial energies is derived:

$$\begin{cases} \sigma_{SV} = \frac{\sigma_{LV}}{2} \left( \sqrt{1 + \sin^2 \theta_0} + \cos \theta_0 \right) \\ (\sigma_{SL})_0 = \frac{\sigma_{LV}}{2} \left( \sqrt{1 + \sin^2 \theta_0} - \cos \theta_0 \right) \end{cases} \quad (6)$$

where  $(\sigma_{SL})_0$  is initial S–L interfacial energy.

Once the values of angle  $\theta_1$  and liquid–vapour interfacial energy ( $\sigma_{LV}$ ) are obtained, the  $\sigma_{SV}$  and  $\sigma_{SL}$  of the equilibrium state will be calculated. Table 1 shows

values of  $\sigma_{LV}$  versus temperature for pure Al at experimental temperatures reported in Ref. [13]. And liquid–vapour surface energies of Cu–Si alloys at temperature between 1373 and 1723 K were measured by KHILYA and IVASHCHENKO [20].

Data of  $\theta_0$  for each wetting system are obtained from those figures (Figs. 2–4) of contact angle versus time, which are shown in Table 2. Then the solid–vapour surface energies ( $\sigma_{SV}$ ) of the graphite are calculated by Eq. (6). A conclusion can be drawn that surface energy of graphite substrate is  $(85 \pm 11)$  mJ/m<sup>2</sup> in this work. And Table 3 shows surface energies of carbon and carbon fibers studied by DONNET et al [21].

**Table 1** Experimental values of  $\sigma_{LV}$  for different liquids

Liquid	$T_F/K$	Experimental $\sigma_{LV}/(mJ \cdot m^{-2})$	Experimental temperature/K	$\sigma_{LV}/(mJ \cdot m^{-2})$
Al	933	$867-0.15(T-T_F)$	1273	801 [13]
Cu-30% Si	—	—	1423	989 [20]
Cu-40% Si	—	—	1423	909 [20]
Cu-50% Si	—	—	1423	853 [20]

**Table 2** Experimental values of  $\sigma_{LV}$ 

Couple	$T/K$	$\sigma_{LV}/(mJ \cdot m^{-2})$	$\theta_0/(^{\circ})$	$\theta_2/(^{\circ})$	$\sigma_{SV}/(mJ \cdot m^{-2})$
Al/C	1273	801	150.79	173.11	96.10
Cu-30% Si/C	1423	989	157.56	175.81	72.25
Cu-40% Si/C	1423	909	155.13	174.91	80.72
Cu-50% Si/C	1423	853	152.46	173.83	91.73

The initial angle ( $\theta_0$ ) for Al, Si and Cu-Si alloys on graphite at the desired testing temperature, and the surface energies ( $\sigma_{SV}$ ) of graphite substrate are calculated by Eq. (6).

**Table 3** Surface energies of different substrates

Substrate	$\sigma_{SV}/(mJ \cdot m^{-2})$	Ref.
Vitreous carbon	$63 \pm 10$	[21]
Highly oriented pyrolytic graphite	$62 \pm 11$	[21]
Carbon fibers	$38 \pm 6$	[21]
Graphite in this work	$85 \pm 11$	This paper

If a couple of spontaneous wetting can be completely wetted in the end, the typical values of  $\theta_1=0$  and  $\theta_2=90^{\circ}$  are obtained at this point with a result occurring of  $\sigma_{LV}=\sigma_{SV}$  and  $\sigma_{SL}=0$ . So, the condition of completely wetting for non-reaction system is that the  $\sigma_{SL}$  equals zero. For  $\sigma_{SV} \leq \sigma_{LV}$ , the range of the  $\sigma_{SL}$  value is  $0 \leq \sigma_{SL} < \sigma_{LV}$ .

In the second stage, it is called as reaction-limited spreading because of chemical kinetics at the triple line being rate-limiting compared with diffusion within the droplet. For the sake of simplicity, it can be divided as three situations.

1) Assuming that the reaction does not change the global drop composition significantly, hence the  $\sigma_{LV}$  is constant with time at the triple line.

2) If the triple line remains on the plane of the substrate so that the  $\sigma_{SV}$  is constant with time as well.

3) Instantaneous contact angle is higher but very close to equilibrium contact angle.

The macroscopic dihedral angle between the L-V interface and S-L interface is divided into two angles at time  $t_1$ ,  $\theta(t_1)$  is angle between the L-V interface and the horizontal line; and  $\theta_E(t_1)$ , called erosion angle, is angle between the S-L interface and the horizontal line. According to the model, we also can transform the infinite system (Fig. 5(c)) to the finite system (Fig. 5(e)).

The angle between the L-V interface and the horizontal line is  $\theta_2(t_1)$  which is related to the  $\theta(t_1)$  on the basis of Eq. (5). In the horizontal and vertical direction of finite system (Fig. 5(e)), the relation of interfacial energies is followed.

$$\begin{cases} \sigma_{SL} \cos \theta_E(t_1) = -\sigma_{LV} \cos \theta_2(t_1) \\ \sigma_{SL} \sin \theta_2(t_1) = \sigma_{LV} \sin \theta_2(t_1) - \sigma_{SV} \end{cases} \quad (7)$$

Equation (7) is simplified as

$$\begin{cases} \tan \theta_E(t_1) = \frac{\sigma_{LV} \sin \theta_2(t_1) - \sigma_{SV}}{-\sigma_{LV} \cos \theta_2(t_1)} \\ \sigma_{SL}(t_1) = -\frac{\cos \theta_2(t_1)}{\cos \theta_E(t_1)} \sigma_{LV} \end{cases} \quad (8)$$

The surface energy has been calculated through the initial angle  $\theta_0$  in Eq. (6), and the surface energy can be known by experiment. The angle  $\theta(t)$  has been measured by a modified sessile drop experiment. For the sake of simplicity, the L-V and S-V surface energies are taken to be unchanged close to the triple line. Then, the  $\sigma_{SL}$  versus time can be obtained as well as  $\theta_E$ .

$$\begin{cases} \sigma_{SV} = \frac{\sigma_{LV}}{2} \sqrt{1 + \sin^2 \theta_0} + \cos \theta_0 \\ \sin 2\theta_2(t) = -\sin^2 \theta(t) \\ \tan \theta_E(t) = \frac{\sigma_{LV} \sin \theta_2(t) - \sigma_{SV}}{-\sigma_{LV} \cos \theta_2(t)} \\ \sigma_{SL}(t) = -\frac{\cos \theta_2(t)}{\cos \theta_E(t)} \sigma_{LV} \end{cases} \quad (9)$$

where  $\theta(t)$  is dynamic contact angle,  $\theta_2(t)$ ,  $\theta_E(t)$  and  $\sigma_{SL}(t)$  are the dynamic transformational angle, dynamic erosion angle and dynamic S-L interfacial energy, respectively.

Calculation results are shown in Fig. 6. In the reaction-limited spreading stage for Al/C system, value and direction of the  $\sigma_{SL}$  vary rapidly with time. The  $\sigma_{SL}$  value decreases from about  $795 \text{ mJ/m}^2$  to  $715 \text{ mJ/m}^2$  with a rate which decreases continuously, while erosion angle increases from  $0^{\circ}$  to  $60^{\circ}$  with a rate which decreases continuously. The diffusion-limited stage is strictly linear, during that the solid-liquid interfacial energy and erosion angle change slightly, and similar changes have been calculated for Cu-Si alloys on graphite.

Additionally, if a couple of reactive wetting can be completely wetted in the end, taking typical values of  $\sigma_{LV}=1000 \text{ mJ/m}^2$ ,  $\sigma_{SV}=400 \text{ mJ/m}^2$  and  $\theta_1=0$ , some values

of  $\theta_2=90^\circ$ ,  $\theta_E=90^\circ$  and  $\sigma_{SL}=600 \text{ mJ/m}^2$  can be obtained. At this point, a result of  $\sigma_{SL}=\sigma_{LV}-\sigma_{SV}=600 \text{ mJ/m}^2$  occurs, so the condition of completely wetting for reaction system is that  $\sigma_{SL}$  equals to the difference between  $\sigma_{LV}$  and  $\sigma_{SV}$ . It has been found that the value of  $\sigma_{SL}$  would reduce during the whole process. For  $\sigma_{SV}\leq\sigma_{LV}$ , the range of the  $\sigma_{SL}$  value is  $\sigma_{LV}-\sigma_{SV}\leq\sigma_{SL}<\sigma_{LV}$ .

With the longer time, the shape of the S–L interface will change to a uniform curvature, as shown in Fig. 5(d). In reaction stage, the erosion angle ( $\theta_E$ ) was changed from the initial angle  $0^\circ$  to final angle ( $\theta_{EF}$ ). And the final angle ( $\theta_F$ ) and ( $\theta_{EF}$ ) are defined by the final interfacial chemistry at the triple line rather than by the intensity of interfacial reactions [22]. Two cases will be considered depending on the difference in wetting.

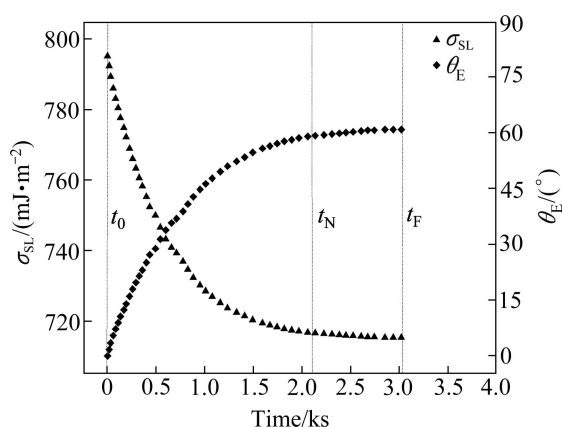


Fig. 6 Solid–liquid surface energy and erosion angle versus time for Al/C system at 1273 K

#### 4.2 Modeling for kinetics

DEZELLUS et al [4,11] introduced a new concept of the surface coverage of the discontinuous product phase  $\alpha$ , and they built the equation of instantaneous contact angle  $\theta(t)$  and the surface coverage  $\alpha$ .

$$\cos \theta_d = \alpha \cos \theta_e + (1 - \alpha) \cos \theta_0 \quad (10)$$

where  $\theta_e$ ,  $\theta_d$  and  $\theta_0$  are respectively the equilibrium, dynamic and initial contact angle.

Then, based on the formula of  $d\alpha/dt = -k(1 - \alpha)$ , it leads to the following equation:

$$\cos \theta_e - \cos \theta_d = (\cos \theta_e - \cos \theta_0) \exp(-k_r t) \quad (11)$$

where  $k_r$  is a dynamic constant, and it represents the spreading rate in the physical meaning. According to this expression, logarithmic plots of  $\cos \theta_e - \cos \theta_d$  versus time would be linear with a slope equal to the kinetic constant  $k$  with opposite sign in reaction-limited spreading stage. Furthermore, most dynamical equations of them had been built on the basis of the relationship between the contact angle or radius and time.

Here, we try to explain problems in reactive wetting by using changes for solid–liquid interfacial energy. Chemical reactions exist at the interface of reactive

wetting systems, and change the physicochemical properties of solid–liquid interface. It can be assumed that the interfacial chemical reaction is a combination reaction.



It is the reducing of interfacial energy in the wetting process that accounts for the spreading of the liquid at the interface. So, there is an assumption that the driving force of wetting process is related with  $\Delta\sigma_{SL}(t)$  which is the difference between instantaneous interfacial energy and final interfacial energy.

$$\Delta\sigma_{SL}(t) = \sigma_{SL}(t) - (\sigma_{SL})_e \quad (13)$$

where  $\sigma_{SL}(t)$  and  $(\sigma_{SL})_e$  are the dynamic and final interfacial energies. The  $\Delta\sigma_{SL}(t)$  value decreases with a rate which decreases continuously in Fig. 6. At the point,  $\Delta\sigma_{SL}(t) \rightarrow 0$ , the driving force will become zero to reach equilibrium state. Based on this assumption, we could describe the rate of interfacial energy,  $d\sigma_{SL}(t)/dt$ , which could describe energy change in reactive wetting, and also reflect the mechanism of reactive wetting. The rate of interfacial energy has two main influence factors. First,  $d\sigma_{SL}(t)/dt$  is in direct proportion to  $\Delta\sigma_{SL}(t)$ ; secondly, the faster the change of the interfacial energy is, the more violent the interfacial reaction is, which leads to the increase of the interfacial reaction rate and the rate of interfacial energy. Based on above assumption, we can roughly describe the rate of interfacial energy change as follows:

$$\frac{d\sigma_{SL}(t)}{dt} = \Delta\sigma_{SL}(t) \cdot v \quad (14)$$

By combining Eqs. (13) and (14), the following expression of  $d\sigma_{SL}/dt$  can be derived:

$$\frac{d\sigma_{SL}(t)}{dt} = [\sigma_{SL}(t) - (\sigma_{SL})_e] v \quad (15)$$

where  $v$  is interfacial reaction rate. According to the experiments of Cu–Si alloys on graphite, the spreading velocity is related to temperature and concentration of active atoms. Assuming that the reactive wetting system is controlled by interfacial chemical reaction, the interfacial reaction rate  $v$  is

$$-v = k C_A^{n_1} C_B^{n_2} \quad (16)$$

For wetting systems in this work, the interfacial reaction is the first-order reaction, and then it has the following formula:

$$-v = kC \quad (17)$$

where  $C$  is concentration of active atoms in the liquid phase, and  $k$  is reaction rate constant which follows the Arrhenius equation:

$$k = k_0 \exp\left(-\frac{E_a}{RT}\right) \quad (18)$$

where  $k_0$  is the pre-exponential factor,  $E_a$  is the apparent activation energy,  $R$  is molar gas constant, and  $T$  is the thermodynamic temperature.

By combining Eqs. (15) and (17), Eq. (19) can be obtained:

$$\frac{d\sigma_{SL}(t)}{dt} = -[\sigma_{SL}(t) - (\sigma_{SL})_e]kC \quad (19)$$

Integrating this equation, the following equation can be produced:

$$\int_{(\sigma_{SL})_0}^{\sigma_{SL}(t)} \frac{1}{\sigma_{SL}(t) - (\sigma_{SL})_e} d\sigma_{SL}(t) = \int_0^t -kC dt \quad (20)$$

It can be simplified as

$$\ln[\sigma_{SL}(t) - (\sigma_{SL})_e] = \ln[(\sigma_{SL})_0 - (\sigma_{SL})_e] - kCt \quad (21)$$

Equation (21) leads to the following expression:

$$\sigma_{SL}(t) - (\sigma_{SL})_e = [(\sigma_{SL})_0 - (\sigma_{SL})_e] \exp(-kCt) \quad (22)$$

where  $(\sigma_{SL})_0$  is the initial interfacial energy, according to this expression, logarithmic plots of  $\sigma_{SL}(t) - (\sigma_{SL})_e$  versus time would be linear with a slope equal to minus  $kC$ .

Figure 7 shows the logarithmic plot of  $\sigma_{SL}(t) - (\sigma_{SL})_e$

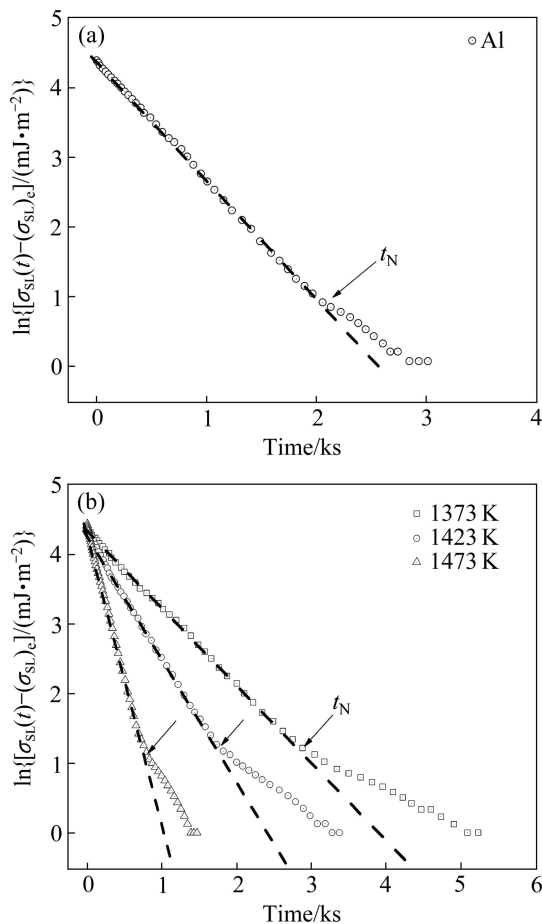


**Fig. 7** Napierian logarithm of  $\sigma_{SL}(t) - (\sigma_{SL})_e$  versus time for Al/C system at 1273 K (a) and for Cu-50% Si alloy/C at different temperatures (b) (The arrows show the sharp change in the slope of these curves at the time  $t_N$ )

as a function of time for Al and Cu-50% Si (mole fraction) alloys on graphite at different temperatures. In the reaction-limited spreading stage, the linear correlation coefficients  $R$  is very close to unity ( $R^2 > 0.99$ ). It must be noted that in order to draw the straight line, a value chosen for  $(\sigma_{SL})_e$  must be a little smaller than the calculation value. For instance, the  $(\sigma_{SL})_e$  value of Al/C system is  $715.48 \text{ mJ/m}^2$ , so  $(\sigma_{SL})_e \approx 714.48 \text{ mJ/m}^2$  was used. Otherwise,  $\sigma_{SL}(t) \rightarrow 715.48 \text{ mJ/m}^2$ , the logarithmic plot of  $\sigma_{SL}(t) - (\sigma_{SL})_e$  is approaching infinity. The values of the fitted parameter  $kC$  as deduced from the slope of the straight line in Fig. 7(b), are  $1.1 \times 10^{-3}$ ,  $1.8 \times 10^{-3}$  and  $4.2 \times 10^{-3}$  respectively, and it must be indicated that an increase in temperature produces a strong acceleration of Cu-50%Si (mole fraction) alloy droplets on graphite. The decrease in chemical-reaction spreading time  $t_N$  is from about 2800 s at 1373 K to 800 s at 1473 K.

## 5 Conclusions

The experimental wetting curves obtained for typical reaction systems can be described in three stages. According to the first stage, the surface energy of graphite is  $(85 \pm 11) \text{ mJ/m}^2$ . The second and the third stages are different types of reactive wetting. In this study, we focus on the kinetics of reaction-limited spreading stage. There is an assumption that the driving force of wetting process is related to  $\Delta\sigma_{SL}(t)$ . The experimental wetting curves obtained for Cu-Si alloys on graphite show that  $d\sigma_{SL}/dt$  is related with Si concentration and temperature. Equations describing spreading in the reaction-limited spreading are derived on the basis of following assumptions.

At any time, the instantaneous  $\sigma_{SL}(t)$  is greater but very close to the equilibrium solid-liquid interfacial energy in the vicinity of the triple line.

The reaction rate is controlled by the process of active atom transferring at the solid-liquid interface. Then a simple equation, such as formula  $\sigma_{SL}(t) - (\sigma_{SL})_e = [(\sigma_{SL})_0 - (\sigma_{SL})_e] \exp(-kCt)$ , is derived for the dependence of  $\sigma_{SL}(t)$ .

The  $k$  is reaction rate constant related to temperature, which follows the Arrhenius equation. The model equations compared with experimental results obtained for pure Al and molten Cu-Si alloys on graphite show good agreement in the reaction-limited spreading stage.

To the authors' knowledge, the above equation is the first time to describe solid-liquid interfacial energy with time in reaction-limited wetting.

## References

- [1] de GENNES P G. Wetting: Statics and dynamics [J]. Reviews of

- Modern Physics, 1985, 57(3): 827–863.
- [2] STAROV V M, VELARDE M G, RADKE C J. Wetting and spreading dynamics [M]. Boca Rato, FL: CRC Press, 2007.
- [3] BLAKE T, HAYNES J. Kinetics of liquid/liquid displacement [J]. Journal of Colloid and Interface Science, 1969, 30(3): 421–423.
- [4] DEZELLUS O, HODAJ F, EUSTATHOPOULOS N. Chemical reaction-limited spreading: The triple line velocity versus contact angle relation [J]. Acta Materialia, 2002, 50(19): 4741–4753.
- [5] MORTENSEN A, DREVET B, EUSTATHOPOULOS N. Kinetics of diffusion-limited spreading of sessile drops in reactive wetting [J]. Scripta Materialia, 1997, 36(6): 645–651.
- [6] YANG L, SHEN P, LIN Q, QIU F, JIANG Q. Effect of Cr on the wetting in Cu/graphite system [J]. Applied Surface Science, 2011, 257(14): 6276–6281.
- [7] ZHANG D, SHEN P, SHI L, JIANG Q. Wetting of B<sub>4</sub>C, TiC and graphite substrates by molten Mg [J]. Materials Chemistry and Physics, 2011, 130(1): 665–671.
- [8] SHEN P, LIN Q, JIANG Q, FUJII H, NOGI K. Reactive wetting of polycrystalline TiC by molten Zr<sub>55</sub>Cu<sub>30</sub>Al<sub>10</sub>Ni<sub>5</sub> metallic glass alloy [J]. Journal of Materials Research, 2009, 24(07): 2420–2427.
- [9] LIN Q, SHEN P, YANG L, JIN S, JIANG Q. Wetting of TiC by molten Al at 1123–1323 K [J]. Acta Materialia, 2011, 59(5): 1898–1911.
- [10] LANDRY K, KALOGEROPOULOU S, EUSTATHOPOULOS N. Wettability of carbon by aluminum and aluminum alloys [J]. Materials Science and Engineering: A, 1998, 254(1): 99–111.
- [11] DEZELLUS O, HODAJ F, EUSTATHOPOULOS N. Progress in modelling of chemical-reaction limited wetting [J]. Journal of the European Ceramic Society, 2003, 23(15): 2797–2803.
- [12] EUSTATHOPOULOS N, NICHOLAS M G, DREVET B. Wettability at high temperatures [M]. Amsterdam: Elsevier, 1999.
- [13] ZHU Ding-yi, WEI Qiao, WANG Ling-deng. Hydrophobic mechanism and criterion of lotus-leaf-like micro-convex-concave surface [J]. Chinese Science Bulletin, 2011, 56(15): 1623–1628. (in Chinese)
- [14] ZHU Ding-yi, LIAO Xuan-mao, DAI Ping-qiang. Theoretical analysis of reactive solid–liquid interfacial energies [J]. Chinese Science Bulletin, 2012, 57(34): 4517–4524. (in Chinese)
- [15] PATANKAR N A. Mimicking the lotus effect: Influence of double roughness structures and slender pillars [J]. Langmuir, 2004, 20(19): 8209–8213.
- [16] WARREN J A, BOETTINGER W, ROOSEN A. Modeling reactive wetting [J]. Acta Materialia, 1998, 46(9): 3247–3264.
- [17] YOST F, SACKINGER P, O'TOOLE E. Energetics and kinetics of dissolutive wetting processes [J]. Acta Materialia, 1998, 46(7): 2329–2336.
- [18] SAIZ E, TOMSIA A P. Kinetics of high-temperature spreading [J]. Current Opinion in Solid State and Materials Science, 2005, 9(4): 167–173.
- [19] AKSAY I A, HOGE C E, PASK J A. Wetting under chemical equilibrium and nonequilibrium conditions [J]. The Journal of Physical Chemistry, 1974, 78(12): 1178–1183.
- [20] KHILYA G, IVASHCHENKO Y N. Free surface energy and density of liquid alloys of the copper–silicon system [C]. Akad Nauk UkrSSR, 1973.
- [21] DONNET J, BRENDLE M, DHAMI T, BAHL O. Plasma treatment effect on the surface energy of carbon and carbon fibers [J]. Carbon, 1986, 24(6): 757–770.
- [22] LANDRY K, RADO C, VOITOVICH R, EUSTATHOPOULOS N. Mechanisms of reactive wetting: The question of triple line configuration [J]. Acta Materialia, 1997, 45(7): 3079–3085.

## 液铝和铜–硅合金的石墨反应润湿动力学

张 弟<sup>1</sup>, 朱定一<sup>1</sup>, 张 腾<sup>1</sup>, 王沁峰<sup>1,2</sup>

1. 福州大学 材料科学与工程学院, 福州 350108; 2. 集美大学 机械与能源工程学院, 厦门 361000

**摘 要:** 为了揭示反应润湿扩散过程的物理本质, 提出一种解释其驱动力和润湿机理的能量模型。在真空条件下采用通管滴落法, 研究熔融的 Al 及 Cu–Si 合金在石墨基板上的反应润湿铺展过程, 由轴对称形状分析软件 (ADSA) 测量摄入图像的接触角。研究典型反应润湿的热力学和动力学过程, 推导能量关系的热力学方程, 计算石墨表面能和三相线处固–液界面能相对于时间的变化值, 并建立关于界面能的动力学模型。借助实验验证该模型的合理性, 表明在反应过程中固液界面能随时间呈指数关系下降。从能量角度可为反应润湿过程提供一种新的解释方法。

**关键词:** 反应润湿; 固–液界面能; 接触角; 石墨; 界面反应

(Edited by Xiang-qun LI)